

# Preliminary Thoughts on Post Collision Diagnostics in CLIC

V. Ziemann

The Svedberg Laboratory, Uppsala University,  
S-75121 Uppsala, Sweden

Draft of November 25, 2003

## **Abstract**

We discuss the properties of the beam after collisions in a 3 TeV center-of-mass CLIC and the possibilities to extract information about the luminosity and other beam dynamical relevant parameters.

## **1 Introduction**

In this note we discuss diagnostic methods to infer properties of the collision process at the IP of a CLIC final focus at 3 GeV center of mass energy. In particular we are interested to have a method to diagnose the luminosity. We start by discussing the properties such as angular divergence and energy spread of the spent beam and then progress on to the discussion of the diagnostic methods, some of them adapted from the SLC final focus, but some new ones as well.

## **2 Beam Properties**

The parameters of the post collision beam in CLIC at 3 TeV can be obtained from D. Schulte's [1] code `GUINEA_PIG`. The input parameters of the simulation are shown in Table 1. The relevant quantities for diagnostic purposes are the angular and energy distribution of the electron and positron beam, both of the primary beams and the coherent pairs. The other quantities of interest are the energy and angular distribution of the beamstrahlung photons.

Table 1: Beam parameters [2]

Energy	1500	GeV
Beam size at IP, $\sigma_x$	60	nm
Beam size at IP, $\sigma_y$	0.7	nm
Bunch length, $\sigma_z$	35	$\mu\text{m}$
RMS momentum spread	0.003	
Crossing angle, $\theta_c$	20	mrad
Crab crossing	yes	

The angular and energy distribution of a primary beam is shown in Fig. 1 and Fig. 2, respectively. We observe that the horizontal angular distribution is double-peaked (why?) and has an rms of about  $140 \mu\text{rad}$ . The vertical distribution is narrower and has a rms of  $20 \mu\text{rad}$ . The energy distribution shows a very pronounced low-energy tail which is due to the copious production of beamstrahlung photons with energies up to the full beam energy.

The angular distribution of the photons has an rms of about  $140 \mu\text{rad}$  horizontally and  $100 \mu\text{rad}$  vertically. The horizontal distribution exhibits shoulders which probably(?) reflect the double peaked structure of the horizontal angular distribution of the primary beam. The energy distribution is shown in Fig. 4 in a logarithmic scale. We observe that the largest number of photons is emitted at low energies, but there exists a significant tail at higher energies. These photons are responsible for the low energy tail of the energy distribution of the primary beam.

The beamstrahlung photons can spontaneously produce  $e^+ e^-$  pairs in the electromagnetic field of the remainder of the oncoming beam. These pairs are called *coherent* and have the angular distribution shown in Fig. 5. The width of the distributions is about  $330 \mu\text{rad}$  horizontally and  $390 \mu\text{rad}$  vertically and quite a bit wider than the primary beam distribution of the distribution of the underlying photon beam. The energy distribution of the coherent pairs is shown in Fig. 6 where we observe a peak at energies of about a tenth of the beam energy with a significant number extending all the way up to the primary beam energy.

### 3 Layout

In order to get a feeling for the geometry of the trajectories of the out-going beams in relation to the last quadrupole of the opposing beam we use the files

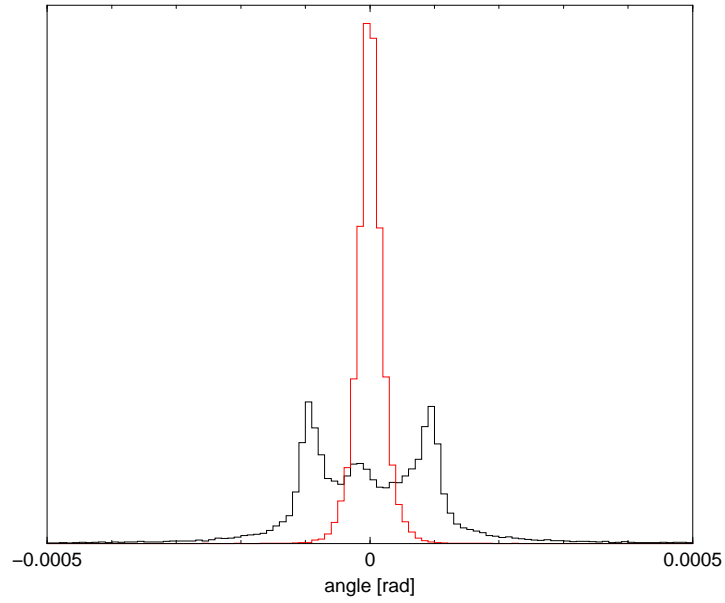


Figure 1: The horizontal (black) and vertical (red) angular divergence of the electron (or positron) beam.

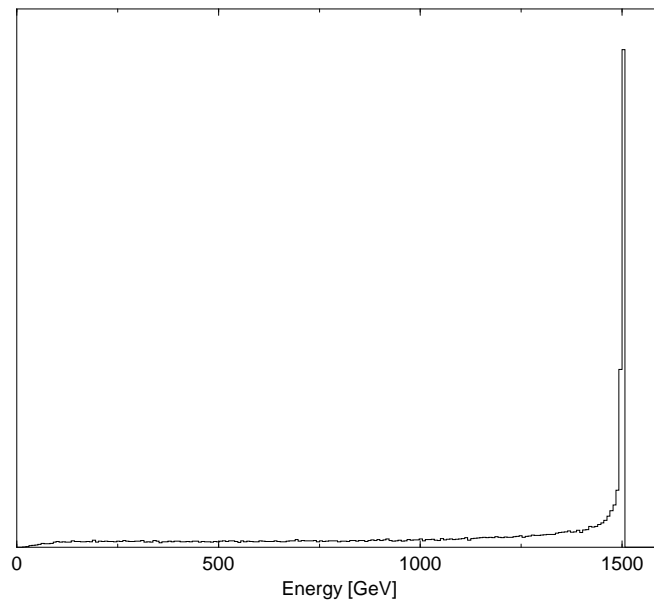


Figure 2: The energy distribution of the electron beam.

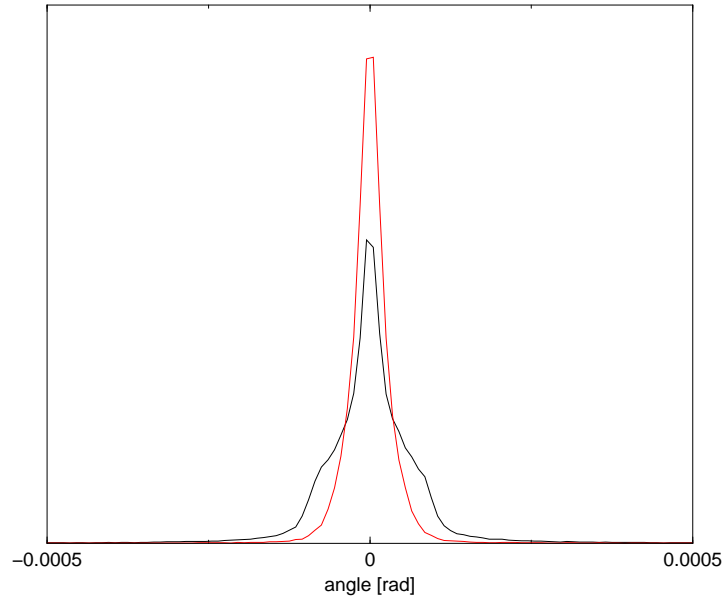


Figure 3: The horizontal (black) and vertical (red) angular distribution of the number of beamstrahlung photons.

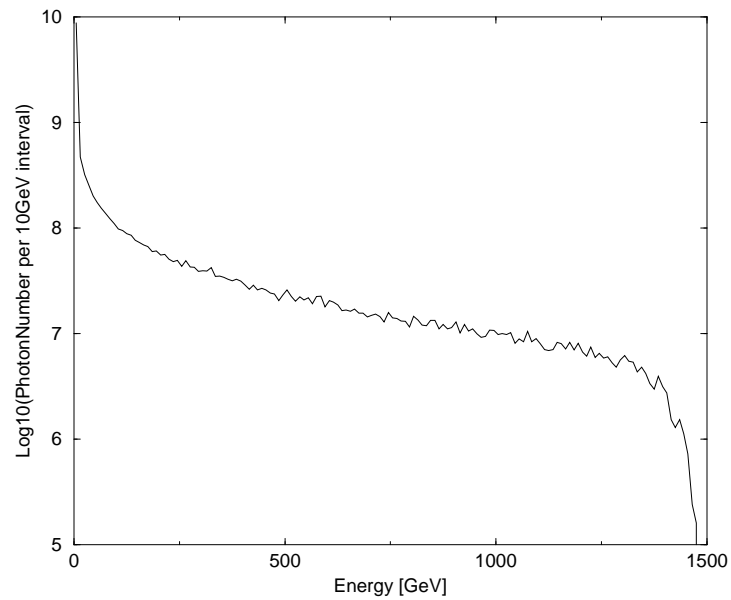


Figure 4: Relative number of beamstrahlung photons as a function of energy.

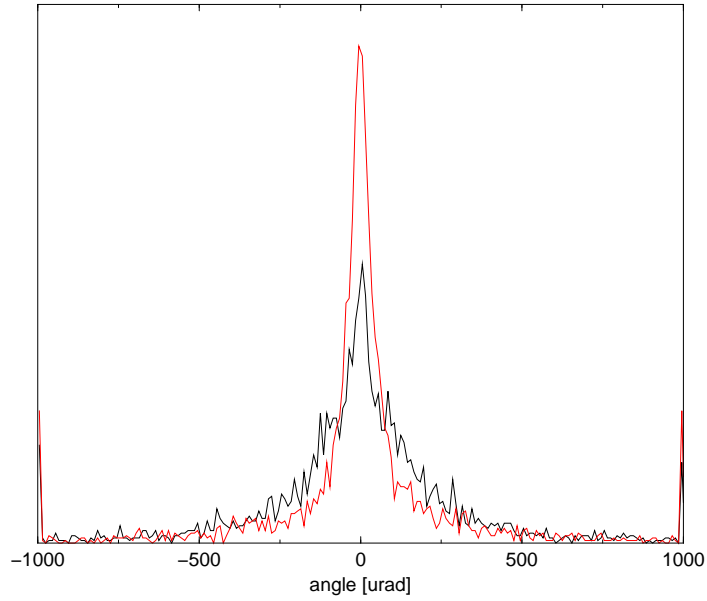


Figure 5: The horizontal (black) and vertical (red) angular distribution of the number of coherent-pair leptons.

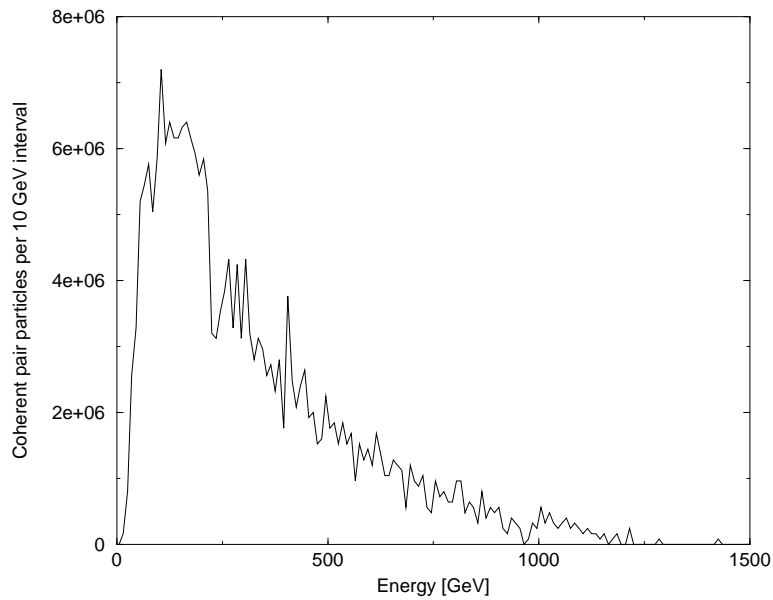


Figure 6: Number of particles in coherent pairs in a 10 GeV interval as a function of energy. Note that only half of the particles are positrons.

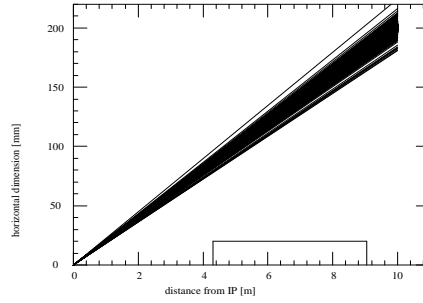


Figure 7: The out-going trajectories from the IP of the primary beam. The last quadrupole seen by the opposing beam is shown in the lower right part of the plot.

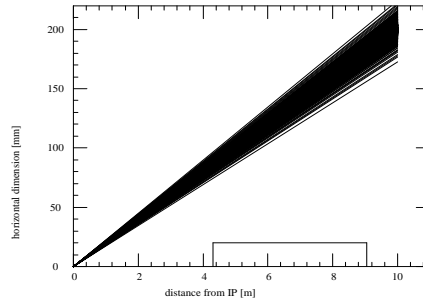


Figure 8: The out-going trajectories of the coherent pairs.

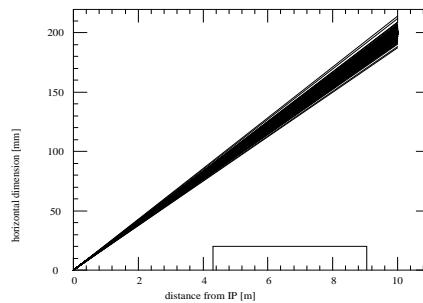


Figure 9: The out-going trajectories of the beamstrahlung photons.

`beam1.dat`, `coh1.dat`, and `photon.dat` that are generated by `GUINEA_PIG`. These files contain the position and angles of the individual particles used in the simulation after the collision. Then it is easy to draw straight lines – ignoring the detector solenoid for the time being – representing the trajectories. Note that we add the 20 mrad crossing angle to the distribution of rays. The quadrupole with a width of 20 mm [3] and length of 4.75 m is shown in the lower right part of the plot showing the trajectories.

In Figures. 7,8, and 9 we show the out-going trajectories. We observe that all particles clear the quadrupole with a good margin and that the coherent pairs have a somewhat larger spread as the photons and the primary beam, which could be expected from the Figures of the previous sections.

## 4 Diagnostics

In this section we discuss mostly diagnostic items that were used in the SLC final focus, but also one new method based on the analysis of the coherent pairs.

### 4.1 Beamstrahlung

From earlier sections we know that most beamstrahlung photons are emitted at low energies where *low* must be seen in relation to the energy of the primary beam. There is, however, also a sizeable fraction of photons at energies up to the full energy. In order to utilize beamstrahlung photons for diagnostic purposes we need to distinguish them from photons generated in static magnetic fields which have a critical energy [4]  $\varepsilon_c$  of

$$\varepsilon_c[\text{GeV}] = 0.665 E^2[\text{TeV}]B[\text{T}] = 1.5 \text{ GeV} \quad (1)$$

in a magnetic field of  $B = 1 \text{ T}$ . This distinction should be quite easy if we focus on photon energies above 10 or 20 GeV. In that case we have to shield the low energy photons and detect the photons that penetrate the shield. In the shielding wall a copious number of secondary products, mostly  $e^+ e^-$ -pairs will be generated and a shower of very fast particles results. These shower products could also serve diagnostic purposes.

The detection of the shower could possibly utilize a similar technique as used in the SLC beamstrahlung monitor built by Clive Field, where the low energy photons are shielded in a tungsten(?) wall, which also causes a shower of rather high energy  $e^+ e^-$ -pairs, which emit Čerenkov radiation in a subsequent gas volume. This radiation is detected by photo tubes. One has to

keep in mind that the radiation levels in CLIC are enormously much higher, such that phot-tubes would not work, such that other detection mechanisms need to be investigated.

Critical parameters in this discussion are the shielding wall material and thickness, the radiation levels and the secondaries that are produced. Furthermore, the placement of this detector is non-trivial, as primary beam has to be separated from the beamstrahlung photons and that one has to avoid back-showering of particles into the detector.

## 4.2 Coherent pairs

Another signal unique to the collision process are coherent pairs, especially the anti-particles of the primary beam traveling into the dump beam line, e.g. the positrons in the electron dump line. As can be seen from Fig. 6 they peak around 150 GeV, so we should design a weak bending magnet that bends the primary electron beam down such that the positrons are bent up by ten times that angle and can be detected, either directly by energy deposition and calorimetry, or using another magnet in which they emit synchrotron radiation that can be detected. The advantage of such a system is that it should rather cleanly only depend on the collision process which is the cause of the positrons.

From Figure 6 we can deduce the approximate synchrotron power that we have to detect. We start by estimating the number of positrons in a 1% bandwidth around 100 GeV which is one tenth of the half of the peak value in Fig. 6 and amounts to about  $3 \times 10^5$  positrons per collision. The pulse is about as long as the primary bunches, namely  $35 \mu\text{m}$ , or  $\Delta t = 0.12 \text{ ps}$ . The bending radius  $\rho$  for a 100 GeV particle in a field of 1 T is about 330 m. If we assume that the magnet is 1 m long we have a bending angle of 3 mrad. Now we can calculate the the peak power by  $\hat{P}$  by [4]

$$\hat{P} = 8.846 \times 10^4 \frac{E^4}{\rho} \hat{I} \times \frac{0.003}{2\pi} = 5 \times 10^6 \text{ W} \quad (2)$$

where  $E$  is the positron energy in GeV and  $\hat{I}$  is the peak current, given by  $\hat{I} = 3 \cdot 10^5 \times 1.6 \cdot 10^{-19} \text{ C} / 0.12 \cdot 10^{-9} \text{ s} = 0.4 \text{ A}$ . The total energy in a single pulse  $U$  is then  $U = \hat{P} \Delta t = 6 \times 10^{-7} \text{ J}$  or  $3.6 \times 10^{12} \text{ eV}$ . Comparing with the critical energy of the photons given by eq. 1 which is 6.6 MeV we find that about  $0.5 \cdot 10^6$  photons are radiated per collision. This should be possible to detect.

A bonus feature of this method is the time resolution, because the time structure of the primary beam is passed on to the coherent pairs which then

emit synchrotron radiation bursts, that can be picked up by a streak camera or some other fast detector.

The separation bend may cause problems and background for the detector, because of the extensive low energy tail of the primary beam and the same-charge half of the coherent beam. These particles hit the wall rather close after the separation bend and may cause excessive background in the detector. This will crucially depend on the distance of the separation bend to the detector.

### **4.3 Vertical double bend**

In SLC there was a double vertical bending magnet in the dump line which caused the emission of synchrotron radiation that was visible as two stripes. This was used to monitor the energy and the energy spread. The extensive low energy tail will probably make this diagnostic item questionable.

### **4.4 Beam-beam deflections**

Another diagnostic method pioneered at SLAC [5] is the analysis of the deflection angle caused by one beam on the other in the collision process. The position can be measured by monitors on either side of the IP and the deflection angle inferred. By scanning one beam across the other and plotting the deflection angle versus the relative offset of the beams the total rms beam sizes and thereby the luminosity together with centering information can be deduced.

Transferring this method to the CLIC final focus will be complicated by at least three effects. First, there is disruption which causes the different longitudinal parts of the beam to get rather different kicks. Second there are the coherent pairs which will induce a signal in the pickup electrodes. This may be a small problem because the pairs will have a zero net charge. Third, when scanning the incoming beam by a steering magnet the position of the beam in the final quadrupoles changes which will cause the beam to receive a transverse kick due to the resistive wall impedance. This effect may be calculated and could in principle be corrected for.

### **4.5 Angular divergence of the spent beam**

The higher the luminosity for a given beam current, the larger the disruption of the out-going beam is. If one could measure the the beam size by e.g. a very thin transition radiation monitor [6] at a certain distance, say, before

the separation bend, one had a measure of the disruption process and thereby the luminosity.

## 5 Conclusions

We discussed the angular divergence and the energy distribution of the different beams emanating from the IP in the CLIC final focus and various methods to infer properties of the colliding beams and the luminosity. Several of the methods are based on experience from SLC and can be adapted to various degrees to CLIC. One novel, rather promising method uses a “weak” vertical bending magnet to separate the opposite-charge companion of the coherent pairs and detects them in another bending magnet by their emitted synchrotron radiation. The signal should be very clean and unique due to the collision process. All involved processes are very fast such that bunch by bunch signals can be deduced. We will investigate this method further in the near future.

## References

- [1] D. Schulte, *Study of Electromagnetic and Hadronic Background in the Interaction Region of the TESLA Collider*, Dissertation, Universität Hamburg, 1996.
- [2] D. Schulte, private communication, November 2003.
- [3] M. Aleksa, et.al., *CLIC Beam Delivery System*, CLIC-Note 551, January 2003.
- [4] A. Chao, M. Tigner, *Handbook of Accelerator Physics and Engineering*, World Scientific, Singapore, 1999.
- [5] P. Bambade, R. Erickson, *Beam-Beam Deflections as an Interaction Point Diagnostic for the SLC*, SLAC-PUB-3979, May 1986.
- [6] P. Piot, et.al., *High-current CW beam profile monitors using transition radiation at CEBAF*, presented at 7<sup>th</sup> beam instrumentation workshop (BIW96) in Argonne II, May 1996.